



# Identification of *KNOP1* as a prognostic marker in hepatocellular carcinoma

Yaping Zhang<sup>1</sup>, Gennian Wang<sup>2</sup>, Mancai Wang<sup>2</sup>

<sup>1</sup>Department of Hepatopathy, Lanzhou University Second Hospital, Lanzhou, China; <sup>2</sup>Department of General Surgery, Lanzhou University Second Hospital, Lanzhou, China

**Contributions:** (I) Conception and design: Y Zhang, G Wang; (II) Administrative support: M Wang; (III) Provision of study materials or patients: Y Zhang, G Wang; (IV) Collection and assembly of data: G Wang; (V) Data analysis and interpretation: All authors; (VI) Manuscript writing: All authors; (VII) Final approval of manuscript: All authors.

**Correspondence to:** Gennian Wang, Master's degree. Department of Hepatopathy, Lanzhou University Second Hospital, 82 Cuiyingmen, Linxia Road, Chengguan District, Lanzhou 730030, China. Email: wgn scholar@126.com.

**Background:** Hepatocellular carcinoma (HCC) is a malignancy with a poor prognosis. This study aimed to evaluate the role and molecular mechanism of lysine-rich nucleolar protein 1 (*KNOP1*) in HCC.

**Methods:** Data from The Cancer Genome Atlas (TCGA), genotype-tissue expression (GTEx), and Gene Expression Omnibus (GEO) databases were used to compare *KNOP1* expression in normal and HCC tissues. The Human Protein Atlas (HPA) database was used to verify *KNOP1* protein expression. Gene Ontology (GO), Kyoto Encyclopedia of Genes and Genomes (KEGG), gene set enrichment, protein-protein and gene-gene interaction network, DNA methylation, genetic alteration, and immune cell infiltration analyses were used to analyze the function and pathway enrichment of *KNOP1*. Finally, receiver operating characteristic (ROC) curves, Kaplan-Meier (KM) analysis, univariate/multivariate Cox regression analyses, and nomograms were used to predict the clinical and prognostic significance of *KNOP1*.

**Results:** *KNOP1* expression was higher in HCC tissue samples than in normal specimens. Additionally, high *KNOP1* expression was positively correlated with T helper 2 (Th2) cells and immune checkpoints. KM analysis, Cox regression analysis, and nomogram prognostic model prediction suggested that high *KNOP1* expression is a risk factor for poor HCC prognosis.

**Conclusions:** *KNOP1* overexpression is associated with poor HCC prognosis and increased proportions of immune cell infiltration and checkpoints. *KNOP1* is a potential biomarker for evaluating HCC prognosis.

**Keywords:** Lysine-rich nucleolar protein 1 (*KNOP1*); hepatocellular carcinoma (HCC); immune cell infiltration; methylation; prognosis

Submitted Jan 01, 2023. Accepted for publication May 30, 2023. Published online Jun 29, 2023.

doi: 10.21037/tcr-23-4

**View this article at:** <https://dx.doi.org/10.21037/tcr-23-4>

## Introduction

Hepatocellular carcinoma (HCC) is the sixth most common type of primary malignancy worldwide, and the fourth leading cause of cancer-related death (1). Current treatment options for liver cancer include surgical resection, interventional therapy, liver transplantation, chemotherapy, and targeted therapy. However, the prognosis of HCC remains poor due to the aggressive, metastatic, and immune

escape characteristics (2). Therefore, there is an urgent need to explore the mechanisms involved in HCC progression and to identify new therapeutic targets that can improve early diagnosis, prognostic assessment, and treatment of HCC.

Lysine-rich nucleolar protein 1 (*KNOP1*) is a nucleolar protein that interacts with zinc finger 106 protein. Also known as Tsg118, it was first reported in 1999 (3). *KNOP1* is predominantly expressed in proliferating somatic cells and in male germ cells, and may therefore be involved in

testicular development (4). However, there have been few investigations of *KNOP1* in HCC. This study analyzed the relationship between *KNOP1* expression and clinical prognosis of HCC with an objective to identify new HCC biomarkers and therapeutic target genes and to generate new ideas for HCC diagnosis and treatment. We present this article in accordance with the Transparent Reporting of a multivariable prediction model for Individual Prognosis or Diagnosis (TRIPOD) reporting checklist (available at <https://tcr.amegrouppublishers.com/article/view/10.21037/tcr-23-4/rc>).

## Methods

### *RNA sequencing (RNA-Seq) data and bioinformatics analysis*

RNA-Seq data in transcripts per million (TPM) format from The Cancer Genome Atlas (TCGA) and genotype-tissue expression (GTEx) databases that were uniformly processed using the Toil process (5) were downloaded from UCSC Xena (<https://xenabrowser.net/datapages/>). RNA-Seq data from the GTEx database (6) and TCGA were integrated to improve the reliability of the results as the sample size of normal tissues in TCGA was small. To further investigate the expression of *KNOP1* in HCC, the expression of *KNOP1* at the messenger RNA (mRNA) and protein levels was verified using data from 2 Gene

Expression Omnibus (GEO; <https://www.ncbi.nlm.nih.gov/geo/>) datasets, namely, GSE55092 (7) and GSE69715 (8), and the Human Protein Atlas (HPA). This study complied with the guidelines issued by TCGA, GEO, and GTEx. Unavailable or unknown clinical information for individual patients included in the study were characterized as missing. The study was conducted in accordance with the Declaration of Helsinki (as revised in 2013).

### *Analysis of differentially expressed genes (DEGs)*

The samples were divided into high and low *KNOP1* expression groups based on the median *KNOP1* expression level. DEGs were identified using the R package DESeq2. The threshold for the DEGs was set at  $|\log_2 \text{fold change (FC)}| > 1.5$  and adjusted  $P < 0.05$  (9).

### *Gene Ontology (GO) and Kyoto Encyclopedia of Genes and Genomes (KEGG) analysis*

DEGs were used for functional enrichment analysis. GO was used to annotate cell composition, including cellular component (CC), molecular function (MF), and biological process (BP). The clusterProfiler package (10) was used for GO and KEGG enrichment analysis of DEGs.

### *Gene set enrichment analysis (GSEA) and analysis of co-expression of cell cycle proteins*

*KNOP1* expression levels were compared using the clusterProfiler package with GSEA to clarify functional and pathway differences. The C2.all.v7.0.symbols.gmt collection in the Molecular Signatures Database (MSigDB) (11) was used as the reference gene collection. Significant enrichment was indicated when  $P < 0.05$ , false discovery rate (FDR)  $< 0.25$ , and  $|\text{normalized enrichment score (NES)}| > 1$ . Spearman's analysis was used to analyze the correlation between *KNOP1* expression and cell cycle proteins.

### *Establishment of protein-protein and gene-gene interaction (GGI) networks*

The Search Tool for the Retrieval of Interacting Genes (STRING) online software (version 11.5) (<http://string-db.org>) was used to predict the protein-protein interaction (PPI) network. Interaction scores were determined by a combined threshold of 0.4 (12). The GGI network was generated using GeneMANIA (<http://genemania.org/>).

### Highlight box

#### Key findings

- *KNOP1* overexpression was associated with poor HCC prognosis and increased proportions of immune cell infiltration and checkpoints.

#### What is known and what is new?

- *KNOP1* is a nucleolar protein that interacts with zinc finger 106 protein, which was first reported in 1999. It is predominantly expressed in proliferating somatic cells and in male germ cells, and may therefore be involved in development of the testes.
- In this study, the results show that *KNOP1* is significantly overexpressed in a variety of tumors, including HCC. *KNOP1* is also associated with pathological stage, histologic grade, tumor status, lower methylation levels, and immune infiltration. High *KNOP1* expression is associated with less favorable overall survival, progression-free interval, and disease-specific survival, which indicates that high *KNOP1* expression may be a significant indicator of poor HCC prognosis.

#### What is the implication, and what should change now?

- *KNOP1* is a potential biomarker for evaluating HCC prognosis.

### *Genetic alterations analysis of HCC patients*

Based on 3 datasets (namely, HCC patients from TCGA, Firehose Legacy; AMC Hepatology 2014 and RIKEN, Nat genet 2012), cBioPortal was used to analyze the genomic profiles of *KNOP1*. The differences between the altered and unaltered *KNOP1* groups were assessed using Kaplan-Meier (KM) plots, and a log-rank test. All P values less than 0.05 were considered statistically significant.

### *Analysis of *KNOP1* gene methylation*

The DNA Methylation Interactive Visualization Database (DNMIVD) (13) (<http://119.3.41.228/dnmivd/index/>) was used to analyze DNA methylation levels of *KNOP1* in HCC and normal tissues from TCGA database. An analysis of promoter methylation levels and *KNOP1* expression was performed using Spearman's correlation. For assessing the relevance of low and high *KNOP1* methylation levels, KM plots were generated and log-rank tests were conducted.

### *Assessment of immune cell infiltration and immune checkpoints*

Immune infiltration analysis was carried out using the single-sample gene set enrichment analysis (ssGSEA) algorithm implemented in the GSVA package (14). A total of 24 infiltrating immune cell types (15) were obtained. A relative enrichment score was calculated for each tumor sample based on its gene expression profile. RNA-Seq expression (level 3) profiles and corresponding clinical information for HCC were downloaded from TCGA database. A total of eight immune checkpoint genes were selected for analysis, including *SIGLEC15*, *TIGIT*, *CD274*, *HAVCR2*, *PDCD1*, *CTLA4*, *LAG3*, and *PDCD1LG2*. Each of these transcripts was analyzed to assess its expression value (16-18). Analysis of *KNOP1*'s correlation with the 24 types of immune cells and checkpoints was performed using Spearman's correlation. A Wilcoxon rank sum test was used to analyze the differences in immune cell infiltration between groups with high and low levels of *KNOP1* expression. The R package ggplot2 (version 3.3.3) was used for data visualization.

### *Clinical analysis of prognostic state*

The patients were divided into high and low expression groups based on the median *KNOP1* expression. To explore

the prognostic value of *KNOP1*, the relationship between *KNOP1* expression and clinical pathologic factors was analyzed using univariate and multivariate Cox regression analyses implemented in the R package survival (version 3.2.10). KM plots were generated and log-rank test was performed to identify differences in overall survival (OS), disease-specific survival (DSS), and progression-free interval (PFI) between the low and high *KNOP1* expression groups. The independent prognostic factors from the multivariate Cox regression analysis were used to construct nomograms and evaluated the 1-, 3-, and 5-year prognostic outcomes. Nomograms were created in R using the rms package, which included calibration plots and significant clinical factors. In order to analyze the calibration curves, the nomogram evaluating probability against actual occurrence was compared to the 45-degree line, which indicates the most accurate prediction. A concordance index (C-index) was analyzed using 1,000 bootstrap resampling steps and the results applied to estimate the discrimination ability of the model. The C-index was used to assess prognostic factors and predictive accuracy of the nomogram. There was a two-tailed statistical test with a significance level of  $P < 0.05$ . The rsm R package (version 6.2.0) was used to generate nomograms and the survminer package (version 0.4.9) was used for visualization.

### *Statistical analysis*

The data were visualized and analyzed using R statistical software (version 3.6.3) (19). Wilcoxon rank sum test was used to evaluate the relationship between *KNOP1* expression and clinical characteristics. KM survival analysis and Cox regression were used to evaluate prognostic factors. Receiver operating characteristic (ROC) curves were generated using the pROC package and used to evaluate the effectiveness of *KNOP1* in distinguishing HCC from healthy samples. The significance of all statistical tests was determined when the two-tailed  $P < 0.05$ .

## **Results**

### ***KNOP1 gene is highly expressed in HCC***

Most tumor types in the databases of TCGA and GTEx were found to have overexpressed *KNOP1* mRNA compared with normal tissue (*Figure 1A*). Among unpaired specimens, *KNOP1* expression was higher in HCC tumor tissues compared with normal tissues from TCGA database

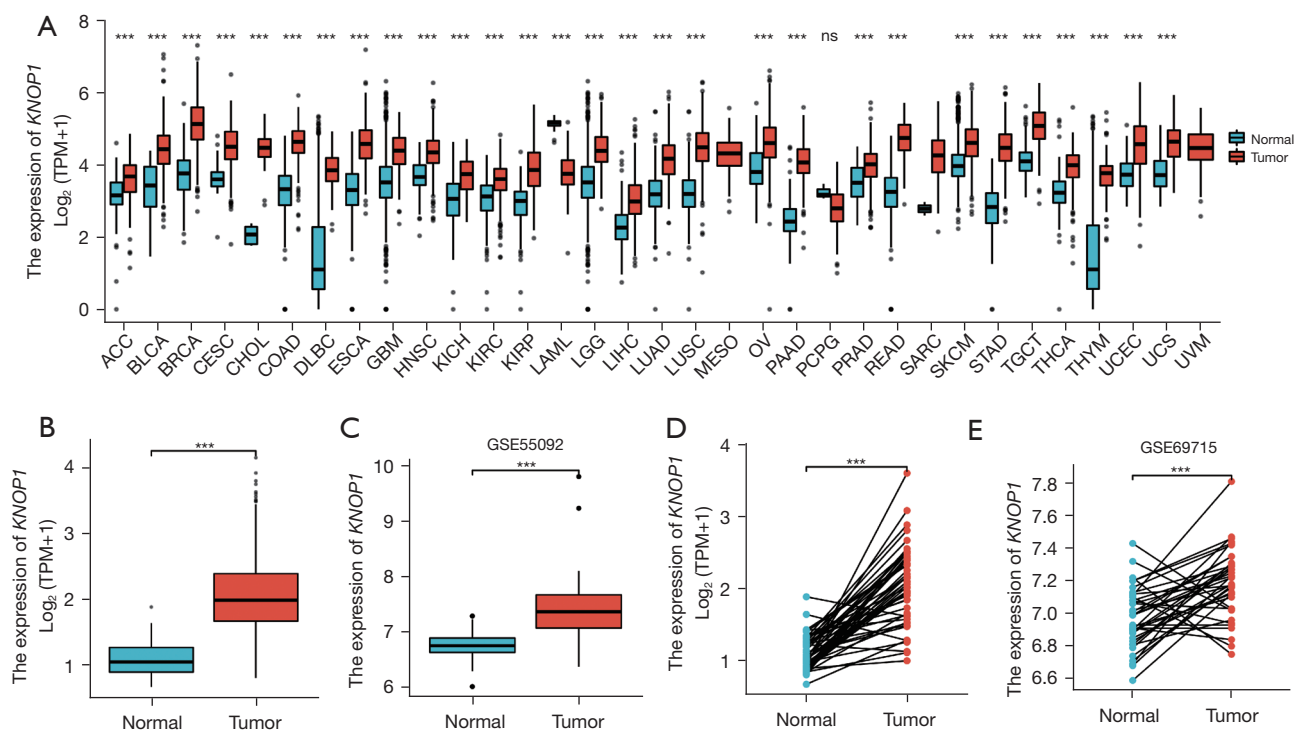


**Figure 1** *KNOP1* expression in patients with HCC. (A) Expression difference of *KNOP1* between tumor and normal tissues in 33 cancer types; (B) expression differences in *KNOP1* between tumor and normal tissues; (C) expression differences in *KNOP1* between tumor and normal tissues in GSE55092; (D) expression differences in *KNOP1* between tumor and paired adjacent tissues; (E) expression differences in *KNOP1* between tumor and paired adjacent tissues in GSE69715. ns,  $P \geq 0.05$ ; \*\*\*,  $P < 0.001$ . *KNOP1*, lysine-rich nucleolar protein 1; TPM, transcripts per million; ACC, adrenocortical carcinoma; BLCA, bladder urothelial carcinoma; BRCA, breast invasive carcinoma; CESC, cervical squamous cell carcinoma and endocervical adenocarcinoma; CHOL, cholangiocarcinoma; COAD, colon adenocarcinoma; DLBC, lymphoid neoplasm diffuse large B-cell lymphoma; ESCA, esophageal carcinoma; GBM, glioblastoma multiforme; HNSC, head and neck squamous cell carcinoma; KICH, kidney chromophobe; KIRC, kidney renal clear cell carcinoma; KIRP, kidney renal papillary cell carcinoma; AML, acute myeloid leukemia; LGG, brain lower grade glioma; LIHC, liver hepatocellular carcinoma; LUAD, lung adenocarcinoma; LUSC, lung squamous cell carcinoma; MESO, mesothelioma; OV, ovarian serous cystadenocarcinoma; PAAD, pancreatic adenocarcinoma; PCPG, pheochromocytoma and paraganglioma; PRAD, prostate adenocarcinoma; READ, rectum adenocarcinoma; SARC, Sarcoma; SKCM, skin cutaneous melanoma; STAD, stomach adenocarcinoma; TGCT, testicular germ cell tumors; THCA, thyroid carcinoma; THYM, thymoma; UCEC, uterine corpus endometrial carcinoma; UCS, uterine carcinosarcoma; UVM, uveal melanoma; HCC, hepatocellular carcinoma.

(Figure 1B) and the GEO database (GSE55029 dataset) (Figure 1C). Among paired specimens, the expression of *KNOP1* mRNA in HCC tissues was significantly higher than in adjacent normal tissues (Figure 1D) and the GEO database (GSE69715 dataset) (Figure 1E).

**Correlation between *KNOP1* expression and clinical pathological features**

Wilcoxon rank sum test was used to compare the difference between *KNOP1* expression in patients with different

clinicopathological features. The results showed that *KNOP1* was associated with tumor-node-metastasis (TNM) stage (Figure 2A-2C), pathological stage (Figure 2D), histologic grade (Figure 2E), tumor status (Figure 2F), Child-Pugh grade (Figure 2G), and vascular invasion (Figure 2H). The OS of patients with HCC was also significantly lower than that of healthy controls (Figure 2I). The HPA database was used to compare the levels of *KNOP1* protein. *KNOP1* protein levels in HCC tissues were higher than in normal tissues (Figure 2J,2K). The ability of *KNOP1* to distinguish HCC patients from healthy

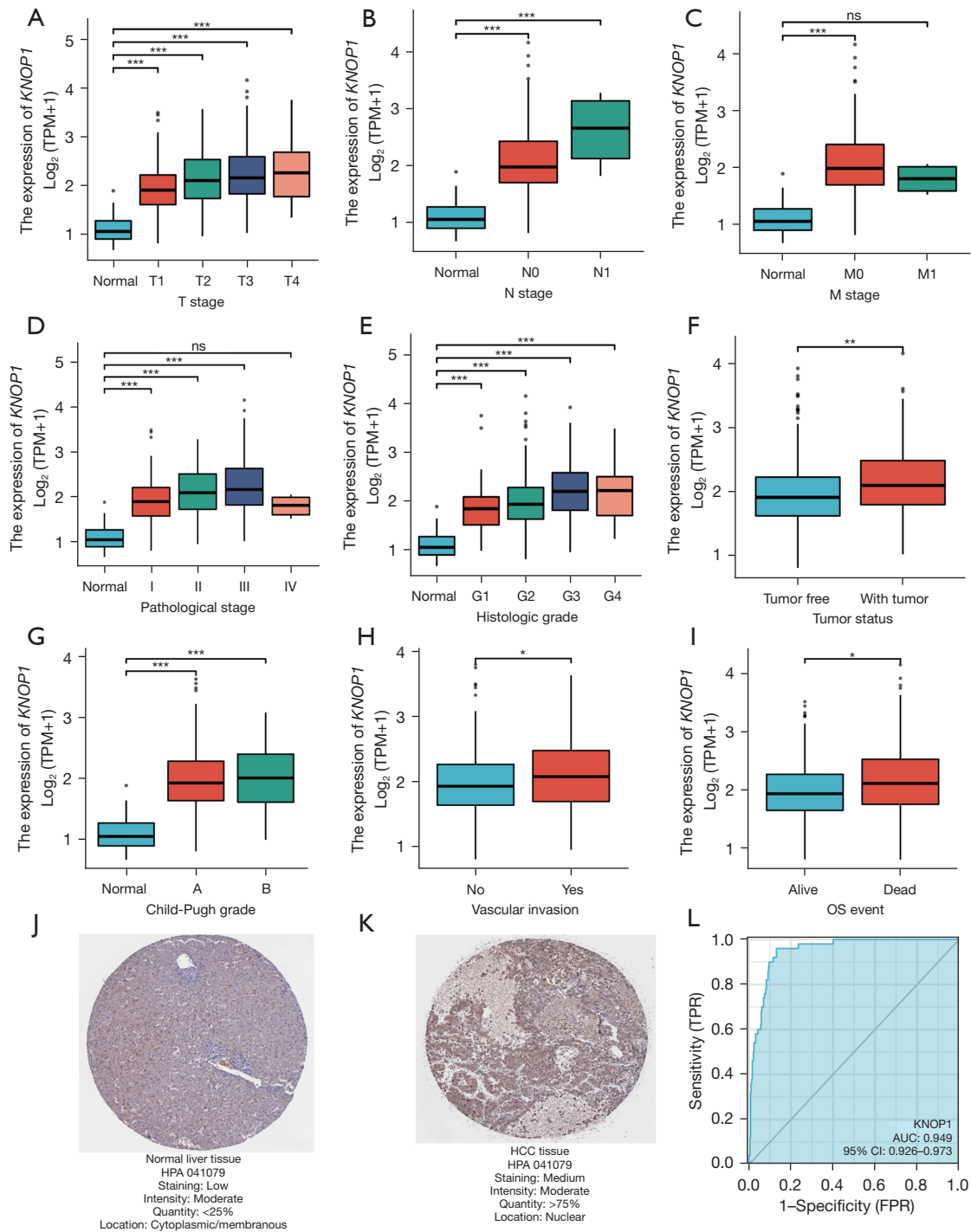


**Figure 2** Associations between *KNOP1* expression and clinicopathological characteristics. The association of *KNOP1* expression and T stage (A); N stage (B); M stage (C); pathologic stage (D); histologic grade (E); tumor status (F); Child-Pugh grade (G); vascular invasion (H); OS event (I). (J,K) The protein expression of *KNOP1* in normal (100×) and HCC tissue (immunohistochemistry staining, 100×) (from HPA: <https://www.proteinatlas.org/ENSG00000103550-KNOP1/tissue/liver>; <https://www.proteinatlas.org/ENSG00000103550-KNOP1/pathology/liver+cancer#img>); (L) ROC curve. ns, P≥0.5; \*, P<0.05; \*\*, P<0.01; \*\*\*, P<0.001. *KNOP1*, lysine-rich nucleolar protein 1; TPM, transcripts per million; FPR, false positive rate; TPR, true positive rate; OS, overall survival; HCC, hepatocellular carcinoma; HPA, Human Protein Atlas; AUC, area under the curve; CI, confidence interval; ROC, receiver operating characteristic.



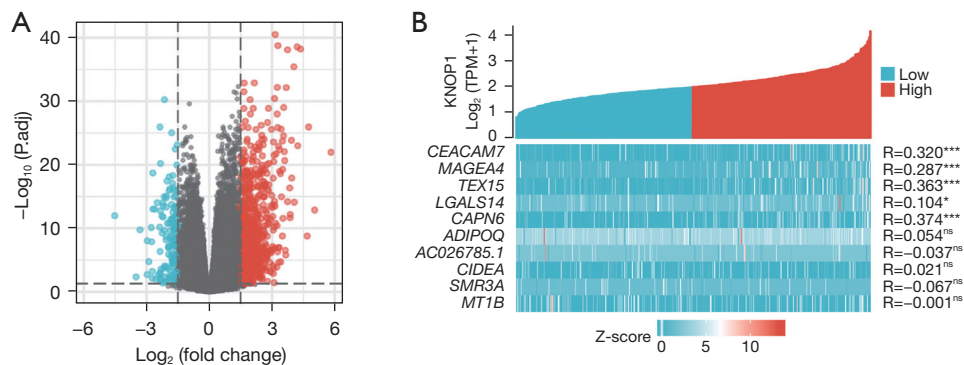


**Figure 3** DEGs in HCC specimen with high and low expression of *KNOPI*. (A) Volcano plot of DEGs. DEGs with markedly down-regulated or up-regulated expression are indicated by blue and red dots, respectively; black dots indicate no significantly changed genes; (B) heatmap of correlation between *KNOPI* expression and the top 10 DEGs. ns,  $P \geq 0.5$ ; \*,  $P < 0.05$ ; \*\*\*,  $P < 0.001$ . *KNOPI*, lysine-rich nucleolar protein 1; TPM, transcripts per million; DEGs, differentially expressed genes; HCC, hepatocellular carcinoma.

individuals was analyzed using ROC curves. The area under the curve (AUC) was 0.949, indicating that *KNOPI* is a potential biomarker (Figure 2L).

#### ***DEGs in HCC specimens with low and high KNOPI gene expression***

The R package DESeq2 was used to analyze HTSeq-count data from TCGA. This study identified 1,102 DEGs (943 upregulated and 159 downregulated) based on the set threshold ( $|\log_2\text{FC}| > 1.5$  and adjusted  $P < 0.05$ ). DEGs were visualized using a volcano plot (Figure 3A) and the top 10 DEGs were represented on a heatmap (Figure 3B).

#### ***GO and KEGG pathway enrichment analysis of DEGs***

GO and KEGG pathway functional enrichment analyses were performed using the clusterProfiler package to better understand the functional significance of the 1,102 genes that were differentially expressed between HCC samples with high and low *KNOPI* expression (Figure 4).

#### ***GSEA of KNOPI gene***

GSEA between low and high *KNOPI* expression datasets was conducted to identify key signaling pathways associated with *KNOPI*. High *KNOPI* expression was associated with DNA replication, cell cycle, and nuclear factor  $\kappa\text{B}$  (NF- $\kappa\text{B}$ ) and T cell receptor signaling pathways (Figure 5). Since the GSEA revealed that *KNOPI* expression was mainly enriched in cell cycle-related pathways, this study

analyzed the correlation between *KNOPI* and cell cycle genes. A Venn diagram of the genes in the KEGG\_CELL\_CYCLE pathway and the KEGG\_DNA\_REPLICATION pathway was created and analyzed the correlation of the 7 genes (*MCM2*, *MCM3*, *MCM4*, *MCM5*, *MCM6*, *MCM7*, and *PCNA*) in the intersection with *KNOPI* (Figure 6A). According to the results, there was a significant and positive correlation between *KNOPI* and all 7 genes (Figure 6B).

#### ***PPI and GGI network analyses***

A PPI network of the top 25 proteins that were correlated with *KNOPI* was generated using the STRING database. The network had 26 nodes (including *KNOPI*) and 97 edges (Figure 7A). A GGI network was generated using GeneMANIA, and the resulting network had 20 genes and 73 links (Figure 7B).

#### ***Genetic alterations in patients with HCC***

The genetic alterations were analyzed using the cBioPortal database. The results showed that the percentage of genetic alterations in *KNOPI* in patients with HCC was 0.8% (Figure 8A), and the difference in disease-free survival between altered and unaltered *KNOPI* groups was statistically significant ( $P = 0.0116$ ) (Figure 8B).

#### ***Methylation of KNOPI gene in HCC patients***

*KNOPI* DNA methylation levels and the correlation between the prognostic value and promoter methylation

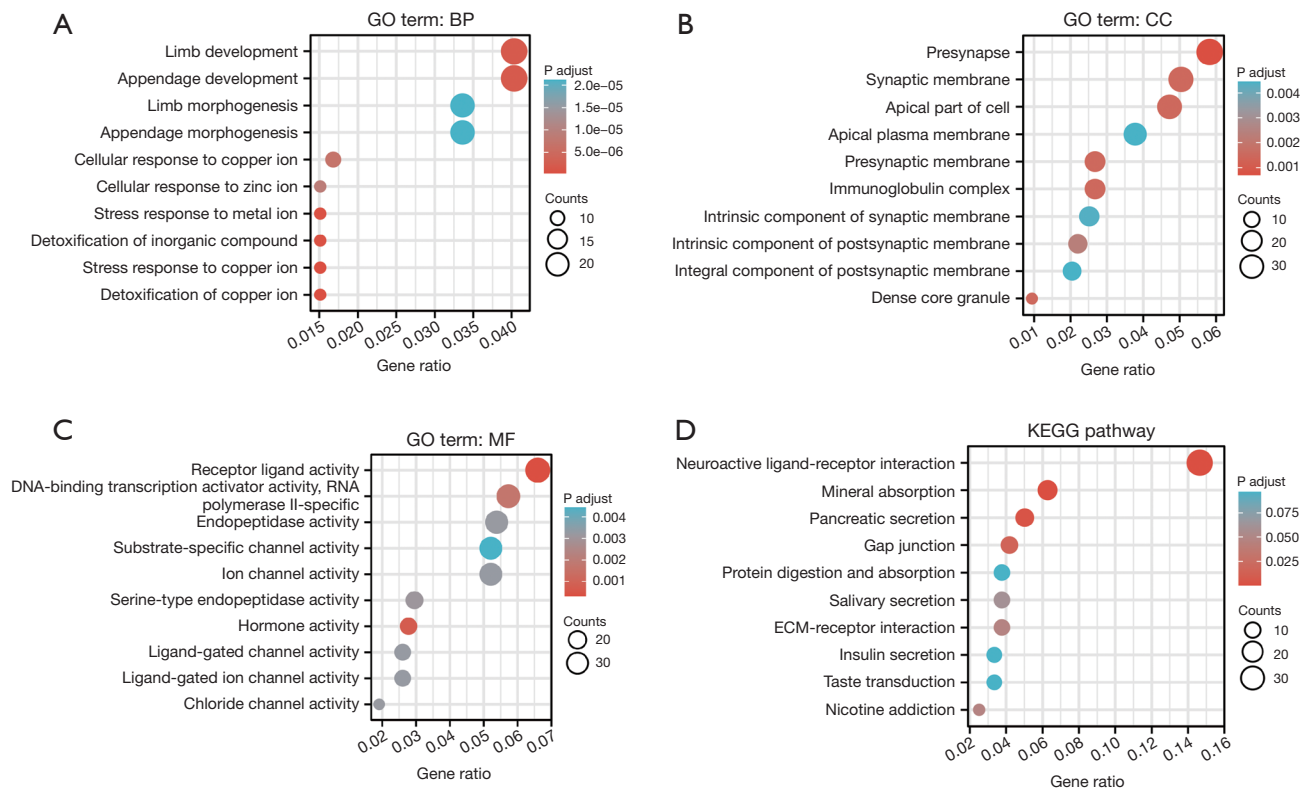


**Figure 4** Functional exploration for *KNOP1* in HCC. (A) GO-BP; (B) GO-CC; (C) GO-MF; (D) KEGG pathways. GO, Gene Ontology; KEGG, Kyoto Encyclopedia of Genes and Genomes; BP, biological process; CC, cellular component; MF, molecular function; ECM extracellular matrix.

levels were investigated using the DNMIIVD database. The results showed that *KNOP1* promoter methylation levels in the tumor group were lower than those in the normal group ( $P < 0.001$ ) (Figure 9A). The methylation level of the *KNOP1* promoter was negatively correlated with *KNOP1* expression (Figure 9B). However, the differences in OS and PFI between patients with low and high *KNOP1* methylation levels were not statistically significant (Figure 9C,9D).

### Infiltration of immune cells in HCC

Based on Spearman's correlation analysis, *KNOP1* expression levels in the HCC microenvironment were associated with immune cell infiltration as measured by ssGSEA. Forest plots showed that *KNOP1* was positively correlated with 11 immune cell subsets, negatively correlated with 12 immune cell subsets, and not correlated with 1 immune cell subset. *KNOP1* was significantly positively correlated with T helper 2 (Th2) cells (Figure 10A). The infiltration levels of Th2 cells were higher in samples in the high *KNOP1* expression

group compared with samples in the low *KNOP1* expression group ( $P < 0.001$ ) (Figure 10B). Explicit *KNOP1* expression was positively related to Th2 cell infiltration ( $r = 0.431$ ,  $P < 0.001$ ) (Figure 10C).

### Analysis of immune checkpoints

This study further analyzed the expression level of 8 immune checkpoints: cluster of differentiation 274 (*CD274*), cytotoxic T-lymphocyte protein 4 (*CTLA4*), hepatitis A virus cellular receptor 2 (*HAVCR2*), lymphocyte-activation gene 3 (*LAG3*), programmed cell death protein 1 (*PDCD1*), prognostic relevance of programmed cell death 1 ligand 2 (*PDCD1LG2*), T cell immunoreceptor with immunoglobulin and ITIM domain (*TIGIT*), and sialic acid-binding immunoglobulin-like lectin 15 (*SIGLEC15*) in HCC and determined the correlation between them. The results showed that the expression levels of *CTLA4*, *HAVCR2*, *PDCD1*, *PDCD1LG2*, *TIGIT*, and *SIGLEC15* were higher in HCC tissues than in normal tissues, whereas

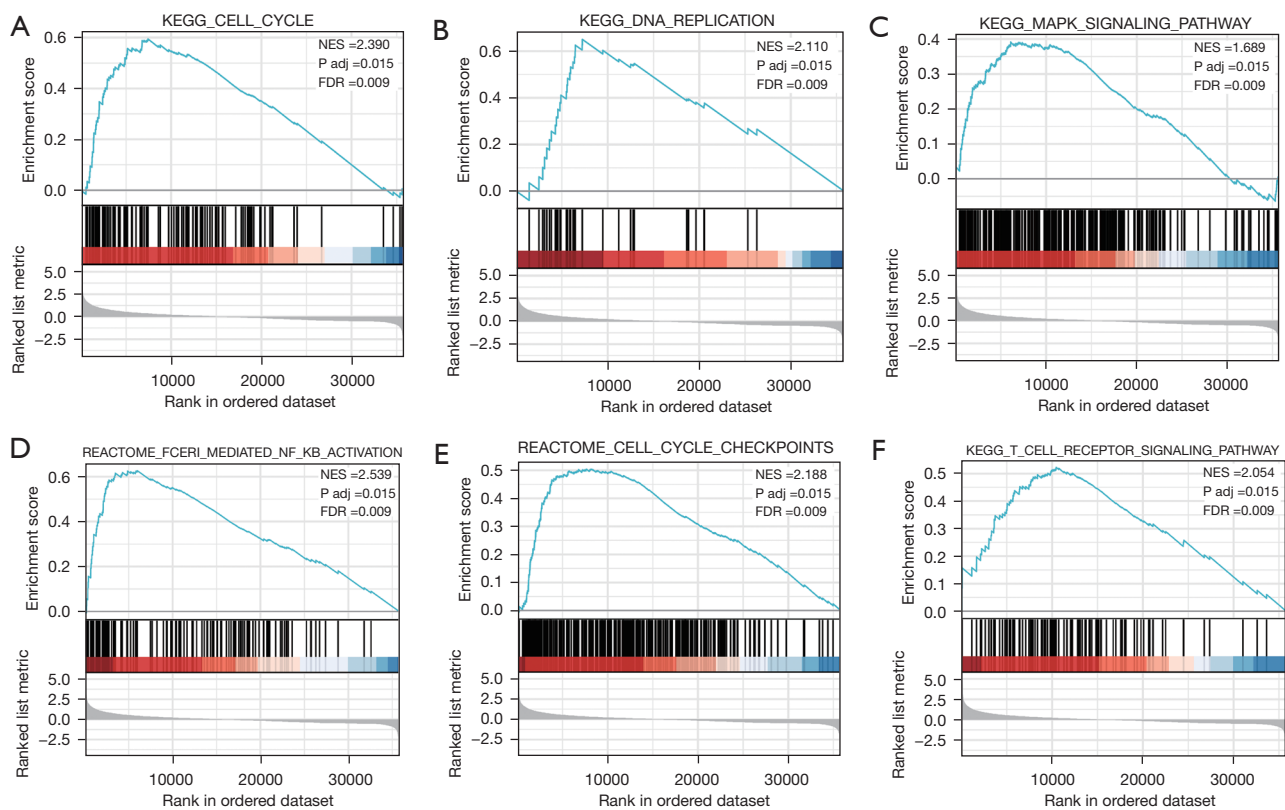


**Figure 5** Functional enrichment of *KNOP1* in HCC by GSEA. (A) Enrichment of genes in cell cycle pathway; (B) enrichment of genes in DNA replication pathway; (C) enrichment of genes in MAPK signaling pathway; (D) enrichment of genes in FCERI-mediated NF- $\kappa$ B pathway; (E) enrichment of genes in cell cycle checkpoints pathway; (F) enrichment of genes in T cell receptor signaling pathway. KEGG, Kyoto Encyclopedia of Genes and Genomes; NES, normalized enrichment score; FDR, false discovery rate; *KNOP1*, lysine-rich nucleolar protein 1; HCC, hepatocellular carcinoma; GSEA, gene set enrichment analysis; MAPK, mitogen-activated protein kinase; NF- $\kappa$ B, nuclear factor  $\kappa$ B; FCERI, Fc epsilon receptor.

the expression levels of *CD274* and *LAG3* were higher in normal tissues than in HCC tissues (Figure 11A). Figure 11B showed the correlation between *KNOP1* and the 8 immune checkpoints in HCC.

### High *KNOP1* gene expression is associated with adverse outcomes in HCC

Data from 250 male and 121 female patients (median age 59 years old) were included in this study. HCC samples were classified into low or high *KNOP1* mRNA expression groups based on the median expression value (2.608 for TPM). A detailed description of the clinicopathological features can be found in Table 1.

KM survival analysis showed that patients with high *KNOP1* expression in TCGA dataset had less favorable OS [hazard ratio (HR) = 1.86, 95% confidence interval

(CI): 1.31–2.64,  $P=0.001$ ; Figure 12A), DSS (HR = 2.63, 95% CI: 1.65–4.20,  $P<0.001$ ; Figure 12B), and PFI (HR = 1.69, 95% CI: 1.26–2.27,  $P<0.001$ ; Figure 12C) compared with patients with low *KNOP1* expression. Univariate and multifactorial Cox regression analyses were used to assess the prognostic factors affecting HCC patients. The results of the univariate Cox regression analysis showed that T3 stage ( $P<0.001$ ), T4 stage ( $P<0.001$ ), pathological M1 stage ( $P=0.018$ ), and high *KNOP1* expression ( $P<0.001$ ) were predictive of poor HCC prognosis. Inclusion of T stage, M stage, and *KNOP1* in a multivariate Cox regression showed that T3 stage ( $P<0.001$ ), T4 stage ( $P=0.006$ ), and high *KNOP1* expression ( $P=0.005$ ) were independent predictors of poor HCC prognosis (Table 2).

To better predict HCC prognosis, the R package rms was used to construct a nomogram to predict the 1-, 3-, and 5-year OS rates of patients with HCC. The model included



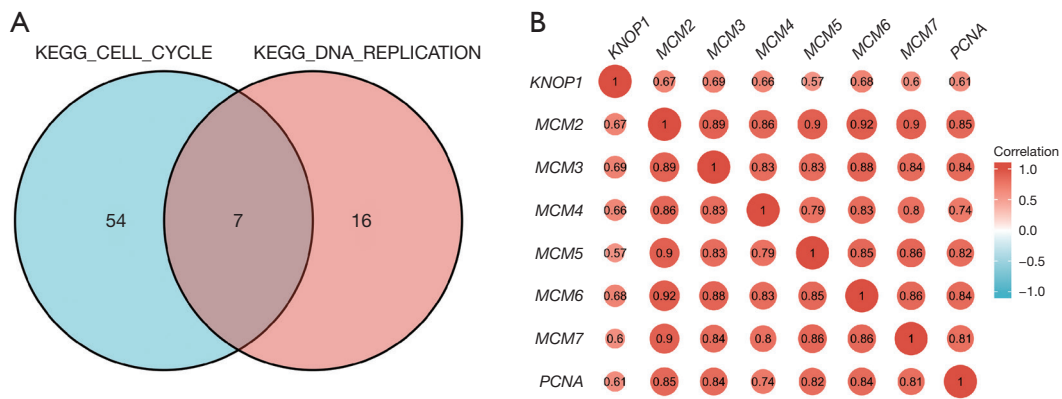


**Figure 6** The correlation between *KNOP1* and cell cycle genes. (A) Venn diagram between genes enriched in KEGG\_CELL\_CYCLE pathway and KEGG\_DNA\_REPLICATION pathway; (B) correlation between *KNOP1* and 7 cell cycle-related genes. *KNOP1*, lysine-rich nucleolar protein 1.

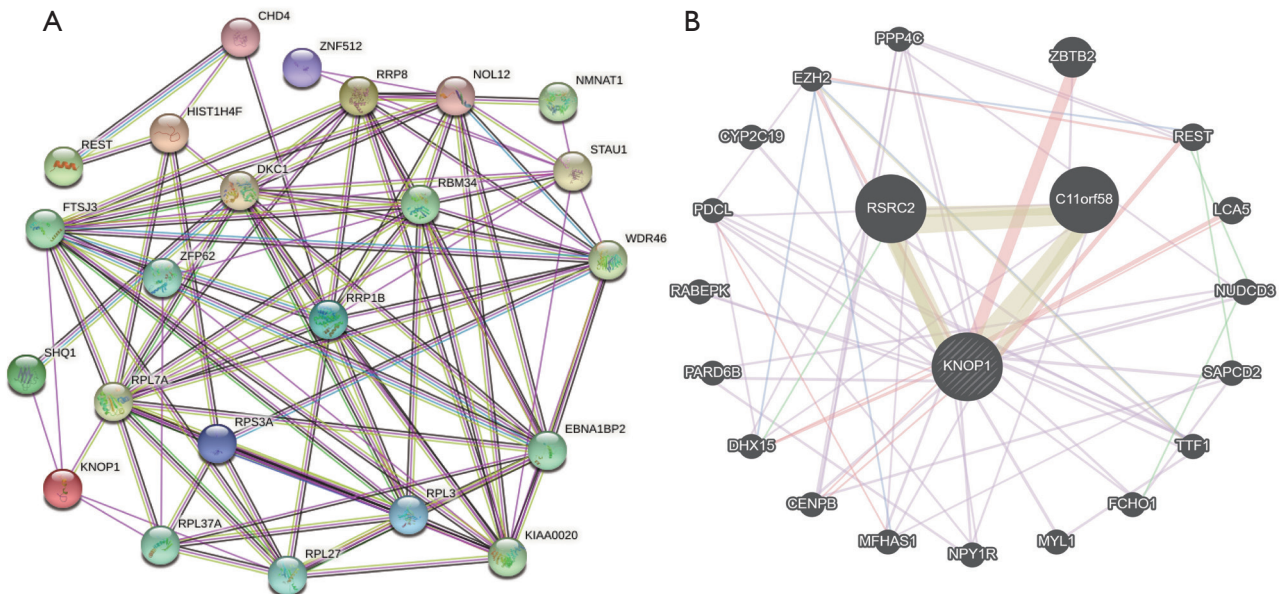


**Figure 7** PPI and GGI networks analysis. (A) The PPI network of top 25 proteins correlated with *KNOP1* drawn by using STRING database; (B) the GGI network associated with *KNOP1* drawn by using GeneMANIA. PPI, protein-protein interaction; GGI, gene-gene interaction; *KNOP1*, lysine-rich nucleolar protein 1; STRING, Search Tool for the Retrieval of Interacting Genes.

5 prognostic variables: T stage, N stage, M stage, age, and *KNOP1* expression. To determine the number of points on these variables, a straight line was drawn upward using a point scale, and a scale of 0 to 100 was applied to each variable's sum of points. Finally, the score of each variable was recorded and the accumulated score taken as the total score. The 1-, 3-, and 5-year OS rates of patients with HCC

were determined by drawing a line from the total point axis straight down to the outcome axis. The results showed that the 1-year OS rate was <30%, and the 3- and 5-year OS rates were <20% for advanced HCC patients. Meanwhile, the 1-, 3-, and 5-year OS for HCC patients in early stage reached up to around 60% (Figure 13A). According to the nomogram calibration curve, the patient observations

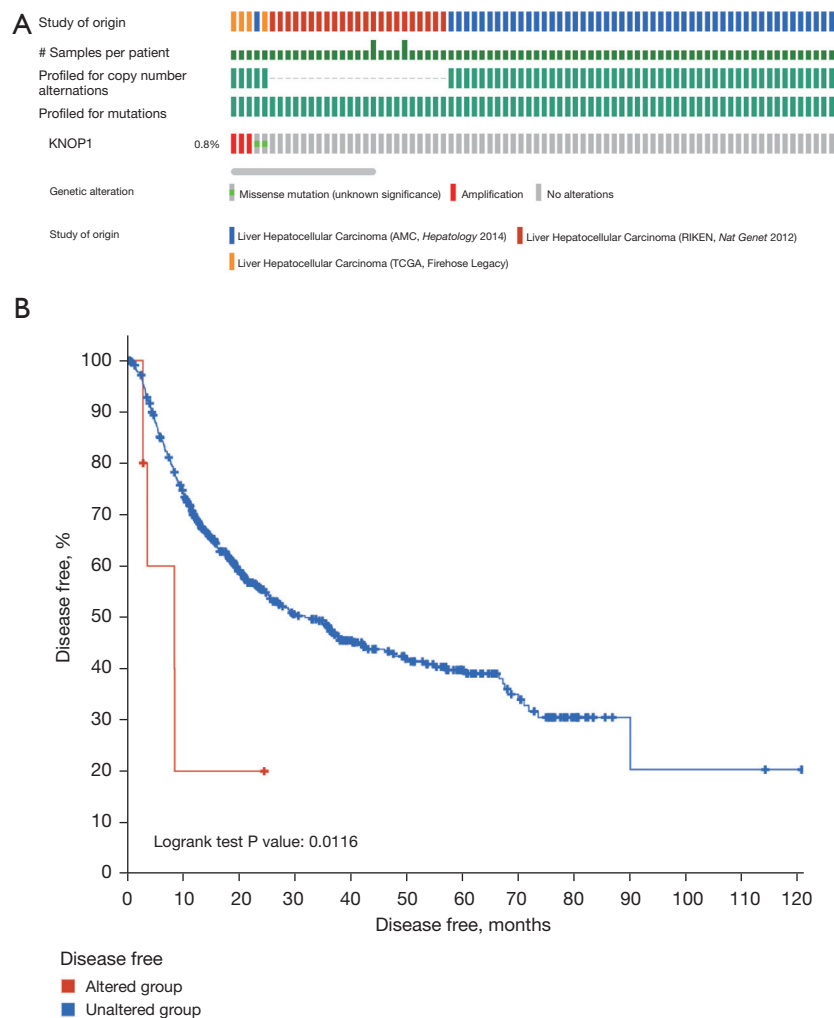


**Figure 8** Genetic alteration of *KNO1* in HCC. (A) OncoPrint visual summary of alteration on a query of *KNO1*; (B) DFS between altered and unaltered groups of *KNO1*. *KNO1*, lysine-rich nucleolar protein 1; AMC, Asan Medical Center; TCGA, The Cancer Genome Atlas; HCC, hepatocellular carcinoma; DFS, disease-free survival.

matched results predicted by the nomogram (*Figure 13B*).

### Discussion

HCC is one of the most common gastrointestinal tumors and is associated with poor prognosis. It is therefore crucial to identify new targets for HCC diagnosis and treatment. Utilizing the TCGA database, this study investigated *KNO1* overexpression in HCC tissues compared to normal liver tissues and showed that high *KNO1* expression was associated with high TNM stage, high pathologic and histologic stages, high Child-Pugh grade, and vascular invasion. In addition, univariate and multifactorial Cox

regression analyses showed that high *KNO1* expression was a significant indicator of poor prognosis. The ability of *KNO1* expression to predict prognosis was further confirmed using a nomogram prediction model, and the calibration plots showed agreement between column line graph predictions associated with *KNO1* and actual observations of 1-, 3-, and 5-year OS probabilities, with individualized scores provided for individual patients. In conclusion, *KNO1* is a potential novel prognostic marker for HCC.

Instability in genomic structure and DNA methylation can lead to cancer development (20). In this study, the percentage of *KNO1* gene alterations in HCC was

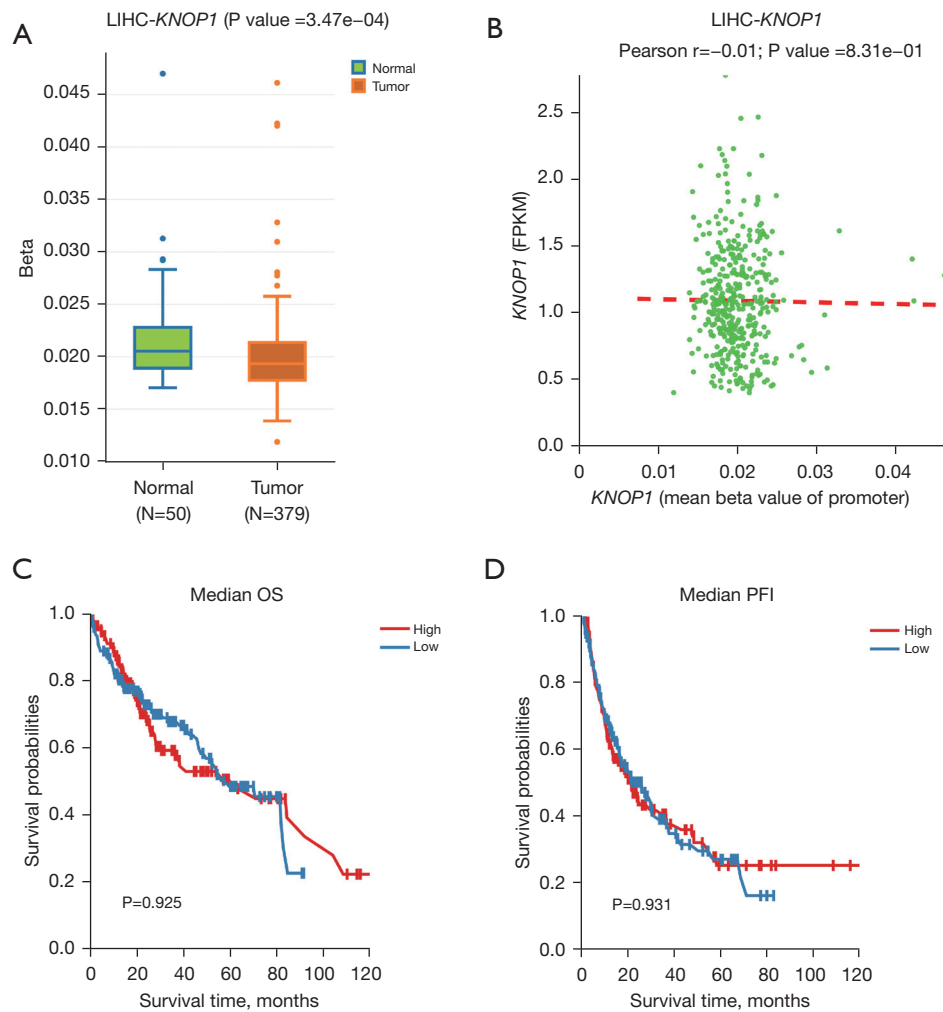


**Figure 9** The analysis of promoter methylation of *KNOP1* in HCC. (A) The promoter methylation levels of *KNOP1* in normal and tumor tissues; (B) methylation of *KNOP1* and its expression; (C) the OS and (D) PFI of the promoter methylation of *KNOP1* in HCC. LIHC, liver hepatocellular carcinoma; *KNOP1*, lysine-rich nucleolar protein 1; FPKM, fragments per kilobase million; HCC, hepatocellular carcinoma; OS, overall survival; PFI, progression-free interval.

approximately 0.8%, but the DSS was higher in the unaltered group compared with the altered group. Analysis of methylation showed that *KNOP1* methylation levels were lower in the tumor group compared with the normal group, but the differences in OS and PFI between patients in the hypermethylated and hypomethylated groups were not statistically significant.

We performed functional enrichment analysis using GO, KEGG, and GSEA to better explore *KNOP1* function. GO analysis showed that high *KNOP1* expression was associated with detoxification of copper ion, stress response to copper ion, detoxification of inorganic compounds, stress response

to metal ion, and cellular response to copper and zinc ion. Several recent studies have shown that alterations in metals such as zinc and copper can modulate molecular targets such as cyclic adenosine-dependent protein kinase (PKA), protein kinase C (PKC), and transcription factors, including NF- $\kappa$ B, that play important roles in the progression and development of various cancers (21,22). Using GSEA, we showed that *KNOP1* was associated with cell cycle, MAPK, and NF- $\kappa$ B related pathways. Several studies have shown that significant enhancement of cell cycle pathways in HCC cells can inhibit the progression of HCC by suppressing the cell cycle (23,24). Abnormal mitotic

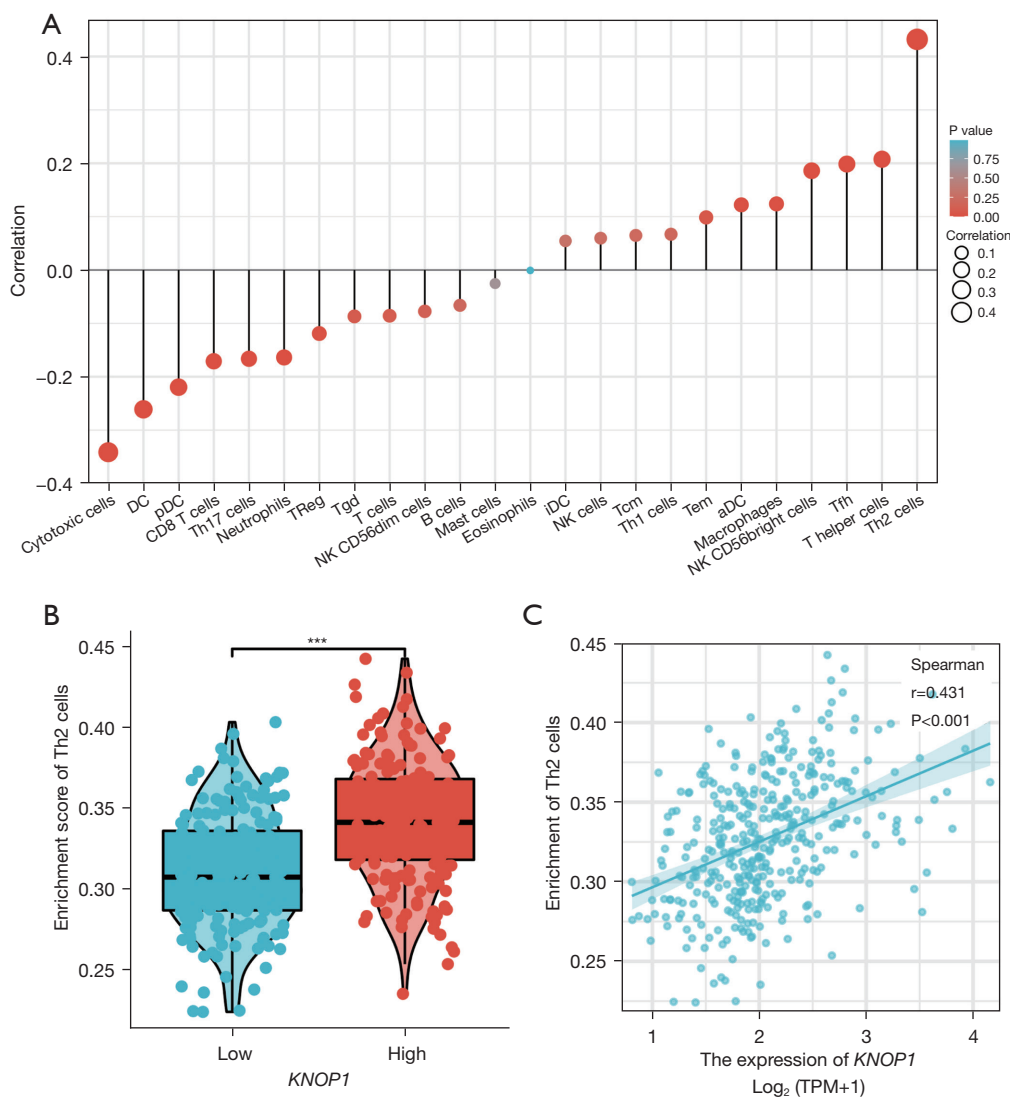


**Figure 10** Correlation analysis between *KNOP1* expression and immune infiltration. (A) Correlation between the relative abundances of 24 immune cells and *KNOP1* expression level; (B) Th2 cells infiltration level in low and high *KNOP1* expression groups; (C) Th2 cells were significantly positively correlated with *KNOP1* expression. \*\*\*,  $P < 0.001$ . *KNOP1*, lysine-rich nucleolar protein 1; DC, dendritic cell; pDC, plasmacytoid pre-dendritic cell; Th17, T helper 17; Treg, regulatory T; Tgd, T gamma delta; NK, natural killer; iDC, immature dendritic cell; Tcm, T central memory; Th1, T helper 1; Tem, T effector memory; aDC, activated dendritic cell; Tfh, T follicular helper; Th2, T helper 2; TPM, transcripts per million.

processes are a key cause of susceptibility and progression of cancers such as HCC. Mitotic errors in HCC progression activate Chk2, resulting in lagging chromosome and DNA damage (25). In addition, mitotic spindles enhance chromosomal instability and HCC progression (25). Microchromosome maintenance families (MCMs) play a central role in replication as replicative DNA helicases, and at least 10 homologs have been identified in humans. Among

them, the *MCM2-7* complex is involved in the formation of pre-replication complexes and exhibits helicase activity (26). *MCM* is a candidate marker of cell proliferation, and elevated levels of *MCM* indicate proliferation of malignant cells. Previous research has shown that mRNA levels of *MCM2*, *MCM6*, and *MCM7* are correlated with certain tumor characteristics and with HCC prognosis (27). In this study, *KNOP1* was significantly and positively correlated

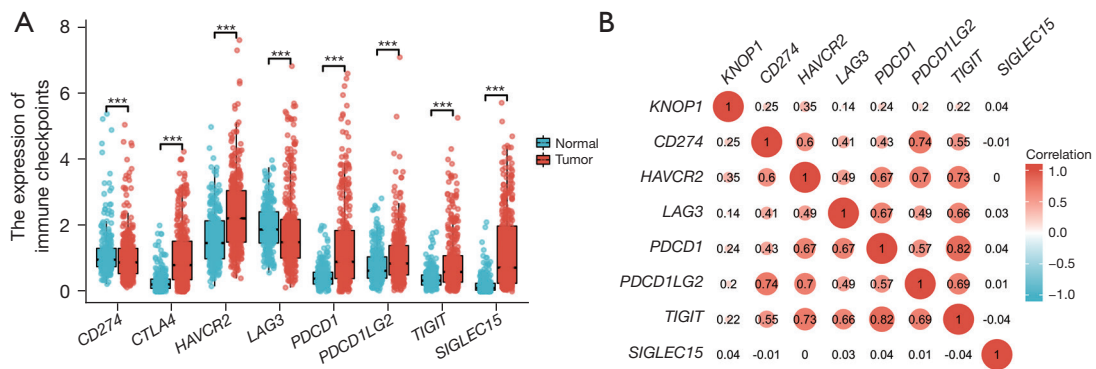


**Figure 11** The analysis of immune checkpoints in HCC. (A) The expression levels of 8 immune checkpoints in HCC and normal tissue; (B) Spearman correlation analysis between *KNOP1* and 8 immune checkpoints. \*\*\*,  $P < 0.001$ . HCC, hepatocellular carcinoma; *CTLA4*: cytotoxic T-Lymphocyte associated protein 4; *HAVCR2*, hepatitis A virus cellular receptor 2; *LAG3*, lymphocyte activating 3; *PDCD1*, programmed cell death 1; *PDCD1LG2*, programmed cell death 1 ligand 2; *TIGIT*, T cell immunoreceptor with Ig and ITIM domains; *SIGLEC15*, sialic acid binding Ig like lectin 15.

**Table 1** The characteristics of HCC patients with high and low *KNOP1* expression in TCGA (n=371)

Characteristics	Low expression of <i>KNOP1</i> (n=185)	High expression of <i>KNOP1</i> (n=186)	P value
Gender, n (%)			0.395
Female	56 (15.1)	65 (17.5)	
Male	129 (34.8)	121 (32.6)	
Age (years), n (%)			0.677
≤60	86 (23.2)	91 (24.6)	
>60	99 (26.8)	94 (25.4)	
AFP (ng/mL), n (%)			0.067
≤400	115 (41.4)	98 (35.3)	
>400	26 (9.4)	39 (14.0)	
T stage, n (%)			0.011
T1	105 (28.5)	76 (20.7)	
T2	40 (10.9)	54 (14.7)	
T3	33 (9.0)	47 (12.8)	
T4	4 (1.1)	9 (2.4)	
N stage, n (%)			0.622
N0	127 (49.6)	125 (48.8)	
N1	1 (0.4)	3 (1.2)	
M stage, n (%)			1.000
M0	135 (50.0)	131 (48.5)	
M1	2 (0.7)	2 (0.7)	

**Table 1** (continued)



Table 1 (continued)

Characteristics	Low expression of <i>KNOP1</i> (n=185)	High expression of <i>KNOP1</i> (n=186)	P value
Pathologic stage, n (%)			0.011
Stage I	100 (28.8)	71 (20.5)	
Stage II	38 (11.0)	48 (13.8)	
Stage III	33 (9.5)	52 (15.0)	
Stage IV	3 (0.9)	2 (0.6)	
Histologic grade, n (%)			0.001
G1	35 (9.6)	20 (5.5)	
G2	98 (26.8)	79 (21.6)	
G3	45 (12.3)	77 (21.0)	
G4	4 (1.1)	8 (2.2)	
Child-Pugh grade, n (%)			0.813
A	117 (49.0)	100 (41.8)	
B	10 (4.2)	11 (4.6)	
C	1 (0.4)	0 (0)	
Fibrosis Ishak score, n (%)			0.994
0	39 (18.4)	35 (16.5)	
1/2	17 (8.0)	14 (6.6)	
3/4	15 (7.1)	13 (6.1)	
5/6	41 (19.3)	38 (17.9)	
Vascular invasion, n (%)			0.088
No	113 (35.9)	93 (29.5)	
Yes	48 (15.2)	61 (19.4)	
Residual tumor, n (%)			<0.001
R0	172 (50.3)	152 (44.4)	
R1	2 (0.6)	15 (4.4)	
R2	1 (0.3)	0 (0)	

HCC, hepatocellular carcinoma; *KNOP1*, lysine-rich nucleolar protein 1; TCGA, The Cancer Genome Atlas; AFP, alpha fetoprotein.

with *MCM2*, *MCM3*, *MCM4*, *MCM5*, *MCM6*, *MCM7*, and *PCNA*, indicating that high *KNOP1* expression may be associated with the proliferation of HCC cells, hence providing a new diagnostic tool for HCC. The MAPK pathway is a ubiquitous signaling pathway involved in many life processes and is frequently altered in many diseases (28). The pathway regulates cellular activities during cancer development, including cell proliferation, apoptosis, and immune escape. Inhibition of the upstream kinases involved

in the MAPK pathway is a therapeutic strategy for some cancers (29).

Tumor-infiltrating immune cells (TIICs) in the immune microenvironment have been associated with immune surveillance and immunotherapy in HCC (30). Th2 cells play an important proto-oncogenic role in tumorigenesis (31), and Lørvik *et al.* (32) suggested that pericyte therapy using tumor-specific Th2 cells may be a highly effective immunotherapeutic option for cancer. In addition, T follicular

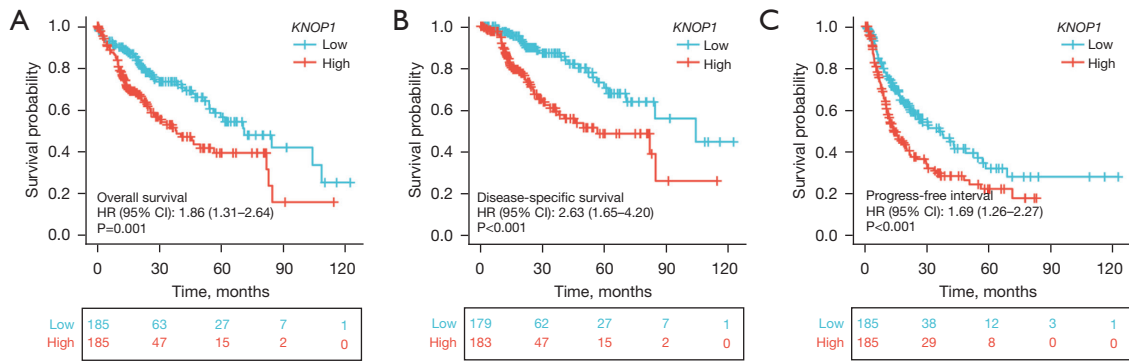


**Figure 12** Kaplan-Meier curve showing overall survival, disease-specific survival, and progression-free interval of HCC patients between low- and high-expression of *KNOP1* from TCGA (A-C). *KNOP1*, lysine-rich nucleolar protein 1; HR, hazard ratio; CI, confidence interval; HCC, hepatocellular carcinoma; TCGA, The Cancer Genome Atlas.

**Table 2** Univariate and multivariate Cox regression analyses of the clinical characteristics associated with overall survival in HCC from TCGA

Characteristics	Total (n)	Univariate analysis		Multivariate analysis	
		Hazard ratio (95% CI)	P value	Hazard ratio (95% CI)	P value
Gender	370				
Female	121	Reference	–	–	–
Male	249	0.816 (0.573–1.163)	0.260	–	–
Age (years)	370				
≤60	177	Reference	–	–	–
>60	193	1.248 (0.880–1.768)	0.214	–	–
T stage	367				
T1	181	Reference	–	Reference	–
T2	93	1.436 (0.906–2.276)	0.124	1.305 (0.718–2.372)	0.382
T3	80	2.615 (1.723–3.970)	<0.001	2.737 (1.635–4.584)	<0.001
T4	13	5.294 (2.644–10.599)	<0.001	4.285 (1.522–12.064)	0.006
N stage	256				
N0	252	Reference	–	–	–
N1	4	2.004 (0.491–8.181)	0.333	–	–
M stage	270				
M0	266	Reference	–	Reference	–
M1	4	4.032 (1.267–12.831)	0.018	1.442 (0.341–6.100)	0.619

**Table 2** (continued)

Table 2 (continued)

Characteristics	Total (n)	Univariate analysis		Multivariate analysis	
		Hazard ratio (95% CI)	P value	Hazard ratio (95% CI)	P value
Histologic grade	365				
G1	55	Reference	–	–	–
G2	177	1.179 (0.696–1.997)	0.541	–	–
G3	121	1.232 (0.710–2.139)	0.457	–	–
G4	12	1.692 (0.625–4.580)	0.301	–	–
AFP (ng/mL)	277				
≤400	213	Reference	–	–	–
>400	64	1.056 (0.646–1.727)	0.827	–	–
Child-Pugh grade	238				
A & B	237	Reference	–	–	–
C	1	2.012 (0.277–14.606)	0.489	–	–
Fibrosis Ishak score	211				
0	74	Reference	–	–	–
1/2	31	0.916 (0.428–1.961)	0.822	–	–
3/4	28	0.681 (0.281–1.654)	0.396	–	–
5/6	78	0.761 (0.424–1.368)	0.361	–	–
Vascular invasion	314				
No	206	Reference	–	–	–
Yes	108	1.348 (0.890–2.042)	0.159	–	–
Residual tumor	341				
R0	323	Reference	–	–	–
R1 & R2	18	1.571 (0.795–3.104)	0.194	–	–
<i>KNOP1</i>	370				
Low	185	Reference	–	Reference	–
High	185	1.856 (1.306–2.637)	<0.001	1.917 (1.222–3.010)	0.005

HCC, hepatocellular carcinoma; TCGA, The Cancer Genome Atlas; CI, confidence interval; AFP, alpha fetoprotein; *KNOP1*, lysine-rich nucleolar protein 1.

helper cells (T<sub>fh</sub>) cells can be differentiated into Th1 and Th2 cells and regulate humoral immune responses (33). Th2 cells can in turn induce the polarization of M1 macrophages into immunosuppressive M2 macrophages (34), leading to the suppression of the host immune system and thus promoting tumorigenesis. In this study, tumor infiltration by Th2 cells, T<sub>fh</sub> cells, and macrophages was positively correlated with *KNOP1* expression, suggesting

that *KNOP1* may play an important role in the regulation of immune infiltrating cells in HCC.

Immune checkpoint inhibitors (ICIs) have revolutionized cancer treatment and led to long term remission in patients with different cancer types (35). Immune checkpoints are involved in the suppression of T-cell or natural killer (NK) cell activation and in the initiation and maintenance of tumor immune tolerance. The best-known ICIs are *CTLA4*

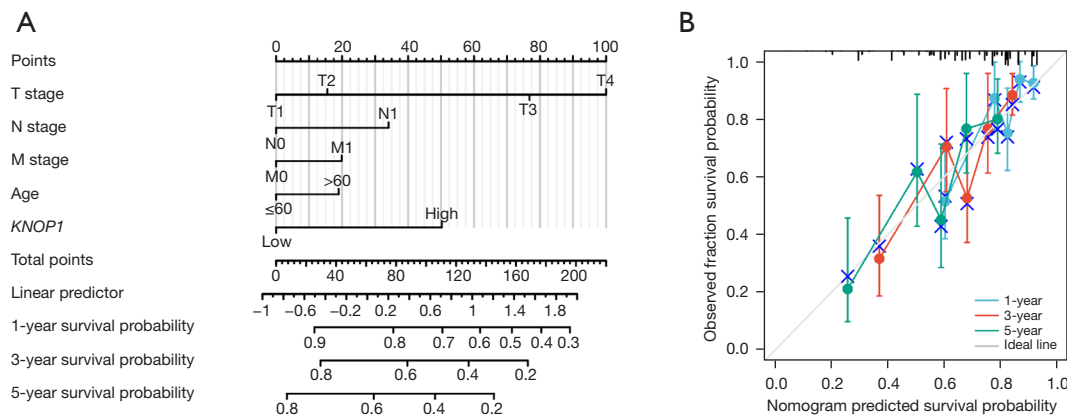


**Figure 13** Establishment of prognosis model. (A) A nomogram to predict the 1-, 3-, and 5-year OS rates of HCC patients; (B) the calibration curve of the nomogram. *KNOP1*, lysine-rich nucleolar protein 1; HCC, hepatocellular carcinoma; OS, overall survival.

and *PDCD1*, which inhibit T cell proliferation and the release of cytotoxic mediators (36,37). We found a positive correlation between *KNOP1* expression and *CTLA4*, *PDCD1*, *HAVCR2*, *PDCD1LG2*, *TIGIT*, *SIGLEC15*, *CD274*, and *LAG3*, suggesting that targeting *KNOP1* may improve the efficacy of ICIs in HCC.

## Conclusions

*KNOP1* was found to play a crucial role in regulating the cell cycle and immune response in HCC. However, this study was limited to *in vitro* investigations, and additional *in vitro* as well as *in vivo* studies are needed to verify the findings herein and to elucidate the specific mechanism of action of *KNOP1* in HCC growth and metastasis in order to determine the clinical applications for patients with HCC.

## Acknowledgments

We would like to thank <https://www.xiantao.love/> for their help in data analysis.

**Funding:** This work was supported by Gansu Youth Science and Technology Fund (No. 21JR1RA149).

## Footnote

**Reporting Checklist:** The authors have completed the TRIPOD reporting checklist. Available at <https://tcr.amegroups.com/article/view/10.21037/tcr-23-4/rc>

**Peer Review File:** Available at <https://tcr.amegroups.com/>

[article/view/10.21037/tcr-23-4/prf](https://tcr.amegroups.com/article/view/10.21037/tcr-23-4/prf)

**Conflicts of Interest:** All authors have completed the ICMJE uniform disclosure form (available at <https://tcr.amegroups.com/article/view/10.21037/tcr-23-4/coif>). The authors have no conflicts of interest to declare.

**Ethical Statement:** The authors are accountable for all aspects of the work in ensuring that questions related to the accuracy or integrity of any part of the work are appropriately investigated and resolved. The study was conducted in accordance with the Declaration of Helsinki (as revised in 2013).

**Open Access Statement:** This is an Open Access article distributed in accordance with the Creative Commons Attribution-NonCommercial-NoDerivs 4.0 International License (CC BY-NC-ND 4.0), which permits the non-commercial replication and distribution of the article with the strict proviso that no changes or edits are made and the original work is properly cited (including links to both the formal publication through the relevant DOI and the license). See: <https://creativecommons.org/licenses/by-nc-nd/4.0/>.

## References

- Villanueva A. Hepatocellular Carcinoma. *N Engl J Med* 2019;380:1450-62.
- D'Avola D, Granito A, Torre-Aláez M, et al. The importance of liver functional reserve in the non-surgical treatment of hepatocellular carcinoma. *J Hepatol*

- 2022;76:1185-98.
3. Larsson M, Brundell E, Jörgensen PM, et al. Characterization of a novel nucleolar protein that transiently associates with the condensed chromosomes in mitotic cells. *Eur J Cell Biol* 1999;78:382-90.
  4. Available online: [https://www.genecards.org/cgi-bin/carddisp.pl?gene=KNOP1#pathways\\_interactions](https://www.genecards.org/cgi-bin/carddisp.pl?gene=KNOP1#pathways_interactions)
  5. Vivian J, Rao AA, Nothhaft FA, et al. Toil enables reproducible, open source, big biomedical data analyses. *Nat Biotechnol* 2017;35:314-6.
  6. Carithers LJ, Moore HM. The Genotype-Tissue Expression (GTEx) Project. *Biopreserv Biobank* 2015;13:307-8.
  7. Melis M, Diaz G, Kleiner DE, et al. Viral expression and molecular profiling in liver tissue versus microdissected hepatocytes in hepatitis B virus-associated hepatocellular carcinoma. *J Transl Med* 2014;12:230.
  8. Sekhar V, Pollicino T, Diaz G, et al. Infection with hepatitis C virus depends on TACSTD2, a regulator of claudin-1 and occludin highly downregulated in hepatocellular carcinoma. *PLoS Pathog* 2018;14:e1006916.
  9. Love MI, Huber W, Anders S. Moderated estimation of fold change and dispersion for RNA-seq data with DESeq2. *Genome Biol* 2014;15:550.
  10. Yu G, Wang LG, Han Y, et al. clusterProfiler: an R package for comparing biological themes among gene clusters. *OMICS* 2012;16:284-7.
  11. Liberzon A, Birger C, Thorvaldsdóttir H, et al. The Molecular Signatures Database (MSigDB) hallmark gene set collection. *Cell Syst* 2015;1:417-25.
  12. Szklarczyk D, Gable AL, Lyon D, et al. STRING v11: protein-protein association networks with increased coverage, supporting functional discovery in genome-wide experimental datasets. *Nucleic Acids Res* 2019;47:D607-13.
  13. Ding W, Chen J, Feng G, et al. DNMIVD: DNA methylation interactive visualization database. *Nucleic Acids Res* 2020;48:D856-62.
  14. Hänzelmann S, Castelo R, Guinney J. GSEA: gene set variation analysis for microarray and RNA-seq data. *BMC Bioinformatics* 2013;14:7.
  15. Bindea G, Mlecnik B, Tosolini M, et al. Spatiotemporal dynamics of intratumoral immune cells reveal the immune landscape in human cancer. *Immunity* 2013;39:782-95.
  16. Ravi R, Noonan KA, Pham V, et al. Bifunctional immune checkpoint-targeted antibody-ligand traps that simultaneously disable TGF $\beta$  enhance the efficacy of cancer immunotherapy. *Nat Commun* 2018;9:741.
  17. Wang J, Sun J, Liu LN, et al. Siglec-15 as an immune suppressor and potential target for normalization cancer immunotherapy. *Nat Med* 2019;25:656-66.
  18. Yi L, Wu G, Guo L, et al. Comprehensive Analysis of the PD-L1 and Immune Infiltrates of m(6)A RNA Methylation Regulators in Head and Neck Squamous Cell Carcinoma. *Mol Ther Nucleic Acids* 2020;21:299-314.
  19. Isidro-Sánchez J, Akdemir D, Montilla-Bascón G. Genome-Wide Association Analysis Using R. *Methods Mol Biol* 2017;1536:189-207.
  20. Mattei AL, Bailly N, Meissner A. DNA methylation: a historical perspective. *Trends Genet* 2022;38:676-707.
  21. Michalczyk K, Cymbaluk-Płoska A. The Role of Zinc and Copper in Gynecological Malignancies. *Nutrients* 2020;12:3732.
  22. Feng Y, Zeng JW, Ma Q, et al. Serum copper and zinc levels in breast cancer: A meta-analysis. *J Trace Elem Med Biol* 2020;62:126629.
  23. Rebouissou S, Nault JC. Advances in molecular classification and precision oncology in hepatocellular carcinoma. *J Hepatol* 2020;72:215-29.
  24. Lee D, Jang MK, Seo JH, et al. ARD1/NAA10 in hepatocellular carcinoma: pathways and clinical implications. *Exp Mol Med* 2018;50:1-12.
  25. Carloni V, Lulli M, Madiati S, et al. CHK2 overexpression and mislocalisation within mitotic structures enhances chromosomal instability and hepatocellular carcinoma progression. *Gut* 2018;67:348-61.
  26. Vijayraghavan S, Schwacha A. The eukaryotic Mcm2-7 replicative helicase. *Subcell Biochem* 2012;62:113-34.
  27. Liu Z, Li J, Chen J, et al. MCM family in HCC: MCM6 indicates adverse tumor features and poor outcomes and promotes S/G2 cell cycle progression. *BMC Cancer* 2018;18:200.
  28. Lee S, Rauch J, Kolch W. Targeting MAPK Signaling in Cancer: Mechanisms of Drug Resistance and Sensitivity. *Int J Mol Sci* 2020;21:1102.
  29. Peluso I, Yarla NS, Ambra R, et al. MAPK signalling pathway in cancers: Olive products as cancer preventive and therapeutic agents. *Semin Cancer Biol* 2019;56:185-95.
  30. Dong LQ, Peng LH, Ma LJ, et al. Heterogeneous immunogenomic features and distinct escape mechanisms in multifocal hepatocellular carcinoma. *J Hepatol* 2020;72:896-908.
  31. Kogame M, Nagai H, Shinohara M, et al. Th2 Dominance Might Induce Carcinogenesis in Patients with HCV-related Liver Cirrhosis. *Anticancer Res* 2016;36:4529-36.
  32. Lorvik KB, Hammarström C, Fauskanger M, et al.



- Adoptive Transfer of Tumor-Specific Th2 Cells Eradicates Tumors by Triggering an In Situ Inflammatory Immune Response. *Cancer Res* 2016;76:6864-76.
33. Rezende RM, Lanser AJ, Rubino S, et al.  $\gamma\delta$  T cells control humoral immune response by inducing T follicular helper cell differentiation. *Nat Commun* 2018;9:3151.
  34. DeNardo DG, Barreto JB, Andreu P, et al. CD4(+) T cells regulate pulmonary metastasis of mammary carcinomas by enhancing protumor properties of macrophages. *Cancer Cell* 2009;16:91-102.
  35. Hiam-Galvez KJ, Allen BM, Spitzer MH. Systemic immunity in cancer. *Nat Rev Cancer* 2021;21:345-59.
  36. Cariani E, Missale G. Immune landscape of hepatocellular carcinoma microenvironment: Implications for prognosis and therapeutic applications. *Liver Int* 2019;39:1608-21.
  37. Lee HW, Cho KJ, Park JY. Current Status and Future Direction of Immunotherapy in Hepatocellular Carcinoma: What Do the Data Suggest? *Immune Netw* 2020;20:e11.

**Cite this article as:** Zhang Y, Wang G, Wang M. Identification of KNOP1 as a prognostic marker in hepatocellular carcinoma. *Transl Cancer Res* 2023;12(7):1684-1702. doi: 10.21037/tcr-23-4